

Supplementary Information

Particle size dependent flexibility in DUT-8(Cu) pillared layer metal-organic framework

Mariia Maliuta,^a Irena Senkovska,^{*, a} Vitaliy Romaka,^{a, ^} Volodymyr Bon,^a Ronja Thümmeler,^{a, ‡} Sebastian Ehrling,^{a, §} Sphi Becker,^{a, ¶} Jack Evans,^{a, #} and Stefan Kaskel^{*, a}

^a Chair of Inorganic Chemistry, Technische Universität Dresden, Bergstraße 66, D-01069 Dresden, Germany

Current affiliations:

[^] Leibniz Institute for Solid State and Materials Research Dresden, Helmholtzstraße 20, 01069 Dresden, Germany

[‡] Leibniz-Institute of Polymer Research Dresden, Hohe Str.6, 01069 Dresden, Germany

[§] 3P INSTRUMENTS GmbH & Co. KG, Rudolf-Diesel-Str.12, 85235 Odelzhausen, Germany

[¶] Gymnasium Wilsdruff, An der Schule 9, 01723 Wilsdruff, Germany

[#] The University of Adelaide, Centre for Advanced Nanomaterials and Department of Chemistry, 5000 Adelaide, Australia

- S1. Experimental details
- S2. Synthesis of DUT-8(Cu) in DEF according to Klein *et al.*
- S3. Desolvation
- S4. Crystal structure
- S5. Adsorption behaviour
- S6. Cluster optimisation
- S7. Thermal analysis
- S8. ¹H NMR Spectroscopy

S1 Experimental details

S1.1 Reagents and solvents

Copper nitrate trihydrate ($\geq 99\%$, AppliChem), 2,6-naphthalene dicarboxylic acid ($H_2(2,6\text{-ndc})$, 99%, Sigma Aldrich), 1,4-diazabicyclo-[2,2,2]-octane (dabco, 99%, Sigma Aldrich), hydrochloric acid (37%, AnalaR NORMAPUR or Sigma Aldrich), *N,N*-dimethylformamide (DMF, 99.5%, Fischer Scientific or Sigma Aldrich), methanol (HPLC grade, HiPerSolv CHROMANORM or VWR Chemicals), ethanol (HPLC grade, HiPerSolv CHROMANORM or VWR Chemicals), DCM (Fischer Scientific, 99.5%), acetone ($\geq 99.5\%$, Sigma Aldrich), 1-propanol (HPLC grade, HiPerSolv CHROMANORM), 1-butanol (HPLC grade, HiPerSolv CHROMANORM).

S1.2 Crystal size modulation and synthesis optimisation

In a typical synthesis, $Cu(NO_3)_2 \cdot 3H_2O$ (0.338 g, 1.4 mmol, 2 eq.), 2,6-naphthalene dicarboxylic acid (0.303 g, 1.4 mmol, 2 eq.), and dabco (0.078 g, 0.07 mmol, 1 eq) were dissolved separately in 5 ml, 15 ml, and 5 ml of DMF, respectively. To suppress fast nucleation, 8.8 ml of HCl solution (1 M in H_2O) was added to the reaction mixture. To study the role of alcohols, four different alcohols were used, namely methanol, ethanol, 1-propanol and 1-butanol. In addition, the ageing temperature was varied from 80 °C over 100 °C to 120 °C (Table S1.1). The DMF/methanol ratio was chosen randomly.

Table S1.1. Utilisation of different alcohols for the synthesis of DUT-8(Cu) at different ageing temperatures.

	methanol	ethanol	1-propanol	1-butanol
80 °C	60 μm	40 μm	40 μm	50 μm
100 °C	60 μm	30 μm	20 μm	20 μm
120 °C	X	20 μm	X	X

X - no product

The evaluation of the resulting materials concerning crystal size was performed by optical microscopy and SEM (Figure S1.2). The highest yield and the largest crystals could be obtained using a DMF/methanol mixture and an ageing temperature of 80 °C. In the next step, the ratio of the starting materials and the solvent was varied.

A variation of the DMF/methanol ratio (batches a-1 - a-3, Table S1.2) leads to the particles up to 100 μm in size, but also to the formation of an additional phase (Figure S 1.1). In the second series of experiments, the dabco content (batches b-1 - b-3, Table S1.2) was varied. The particle size could be further increased using an excess of dabco for the synthesis (Figure S1.2). In addition, the side phase obtained in batches a-1 - a-3 is not present in b-1 - b-3. If the $H_2(2,6\text{-ndc})$ concentration is varied (batches c-1 - c-4) also large particles (ca. 50 μm , Figure S1.2) can be obtained. However, only when an equimolar ratio is chosen, a phase pure product is obtained. In the final step, the ratio between dabco and $H_2(2,6\text{-ndc})$ was kept equal and copper was used as a limiting variable (batch d-1). Interestingly, within this experiment, the biggest crystals with a narrow size distribution could be obtained (Figure S 1.2).

Table S1.2. Synthetic parameters for the synthesis of **2** at 80 °C during 48 hours.

Batch	Cu ²⁺ / mmol	H ₂ (2,6-ndc) / mmol	dabco / mmol	equiv.	DMF / mL	MeOH / mL
a-1	0.4	0.4	0.2	2:2:1	4.5	3.5
a-2	0.4	0.4	0.2	2:2:1	6	2
a-3	0.4	0.4	0.2	2:2:1	3	5
b-1	0.4	0.4	0.1	2:2:0.5	4.5	3.5
b-2	0.4	0.4	0.3	2:2:1.5	4.5	3.5
b-3	0.4	0.4	0.4	2:2:2	4.5	3.5
c-1	0.4	0.467	0.2	2:2.3:1	4.5	3.5
c-2	0.4	0.33	0.2	2:1.65:1	4.5	3.5
c-3	0.4	0.267	0.2	2:1.335:1	4.5	3.5
c-4	0.4	0.2	0.2	2:1:1	4.5	3.5
d-1	0.2	0.4	0.2	1:2:1	6.4	1.75

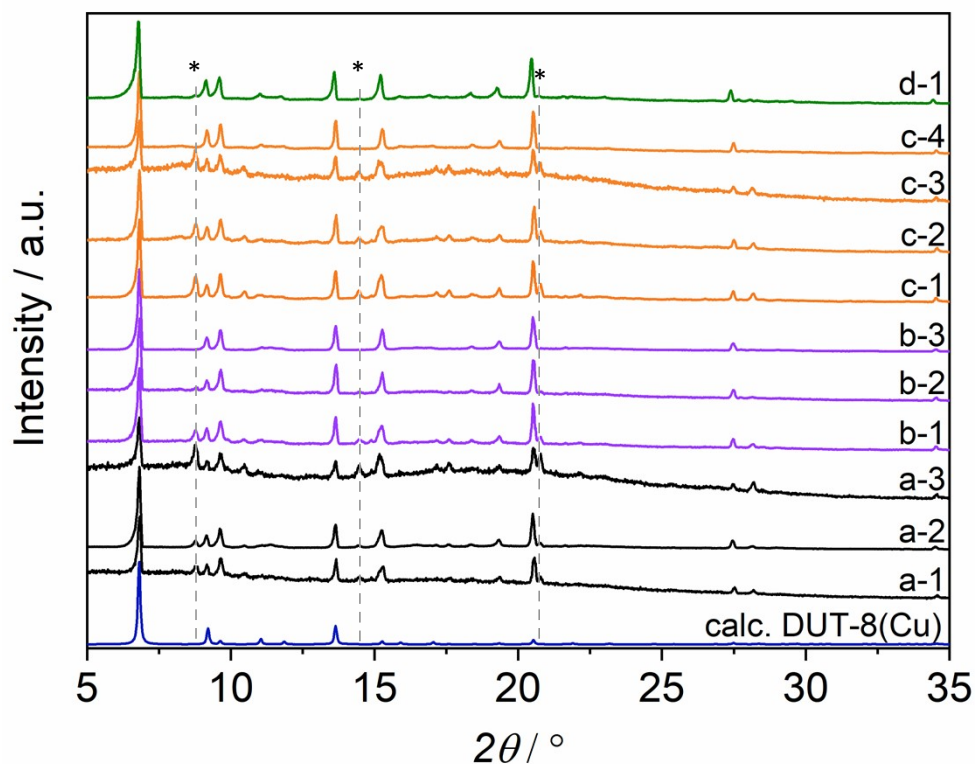


Figure S1.1. PXRD patterns of samples obtained in the synthesis optimisation studies. The peaks of the secondary phases are marked by *.

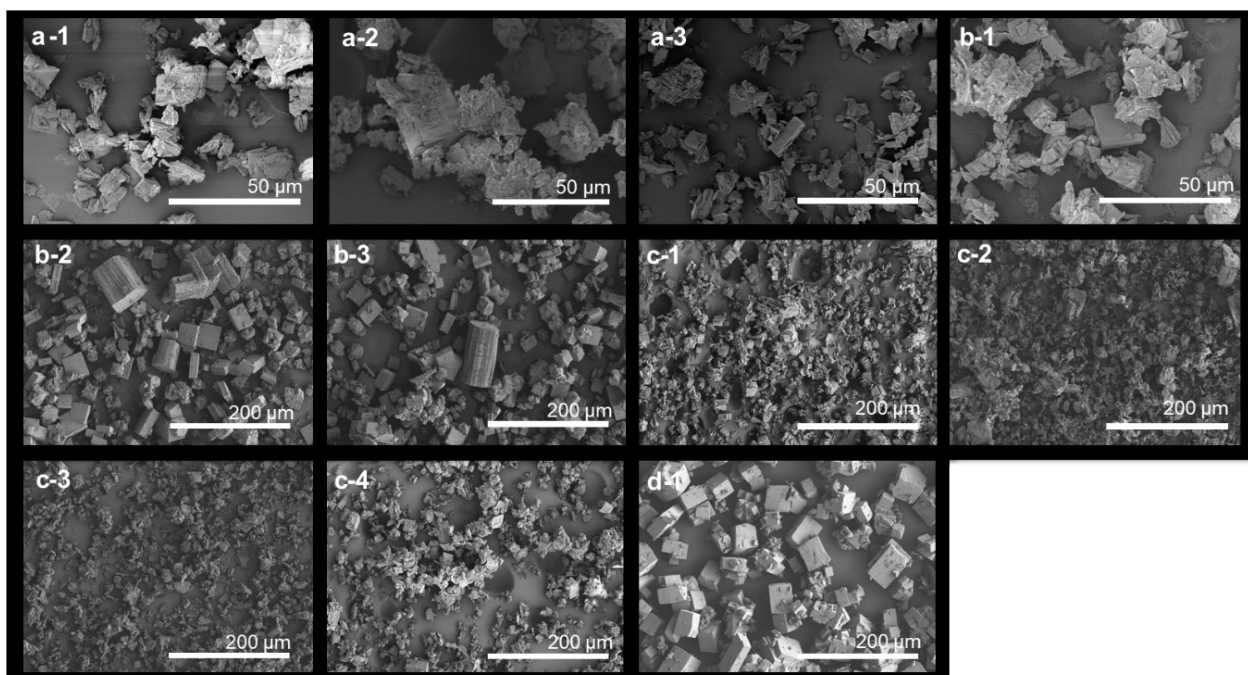


Figure S1.2. SEM images of the crystals obtained in the synthesis optimisation studies.

S2 Synthesis of DUT-8(Cu) in DEF according to Klein *et al.*¹

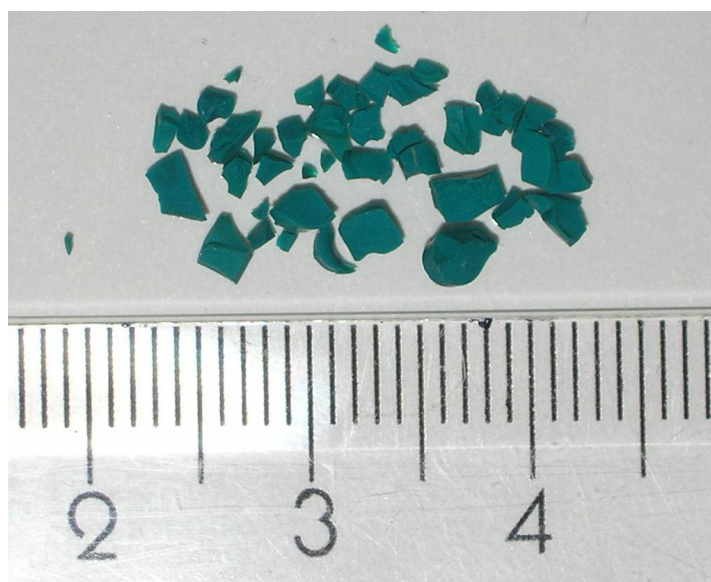


Fig. S2.1. Microscopy image of the DUT-8(Cu) monolith-like solid obtained after drying of the product at 120 °C for 36 h in 2012.²

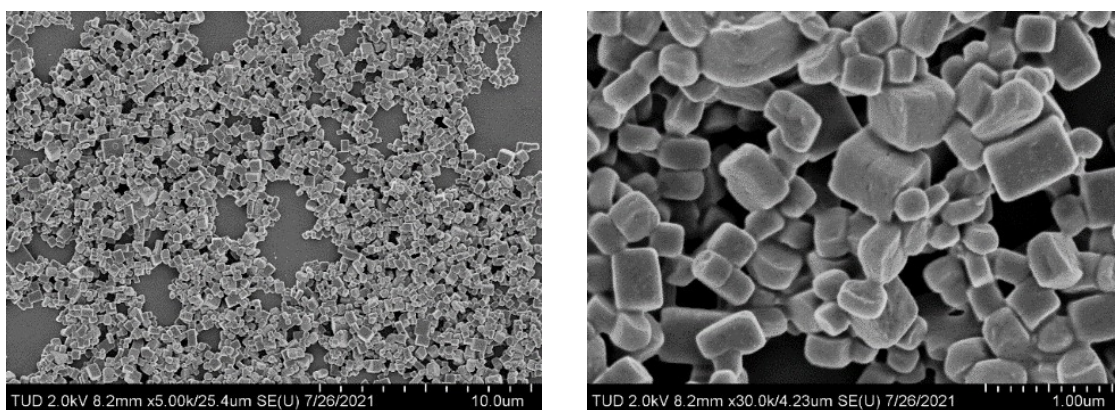


Fig. S2.2. SEM images of the DUT-8(Cu) crystals obtained upon the synthesis in DEF (**1a**), following a synthetic procedure published in 2012.¹

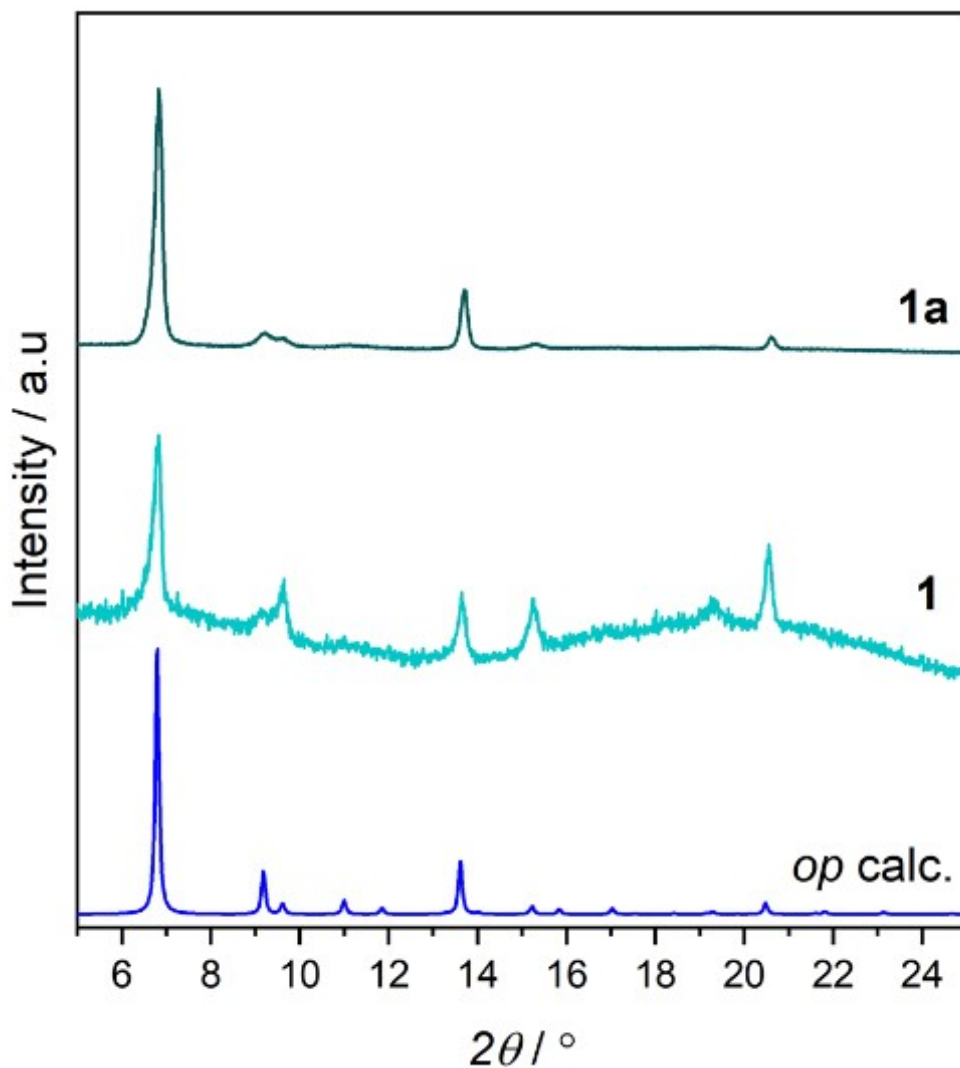


Fig. S2.3. PXRD patterns of **1** and **1a**.

S3 Desolvation

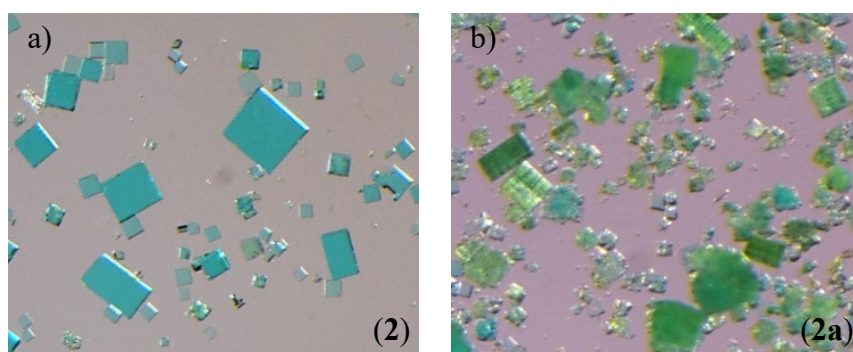


Fig. S3.1. Colour changes of sample **2** upon evacuation: a) before, b) after.

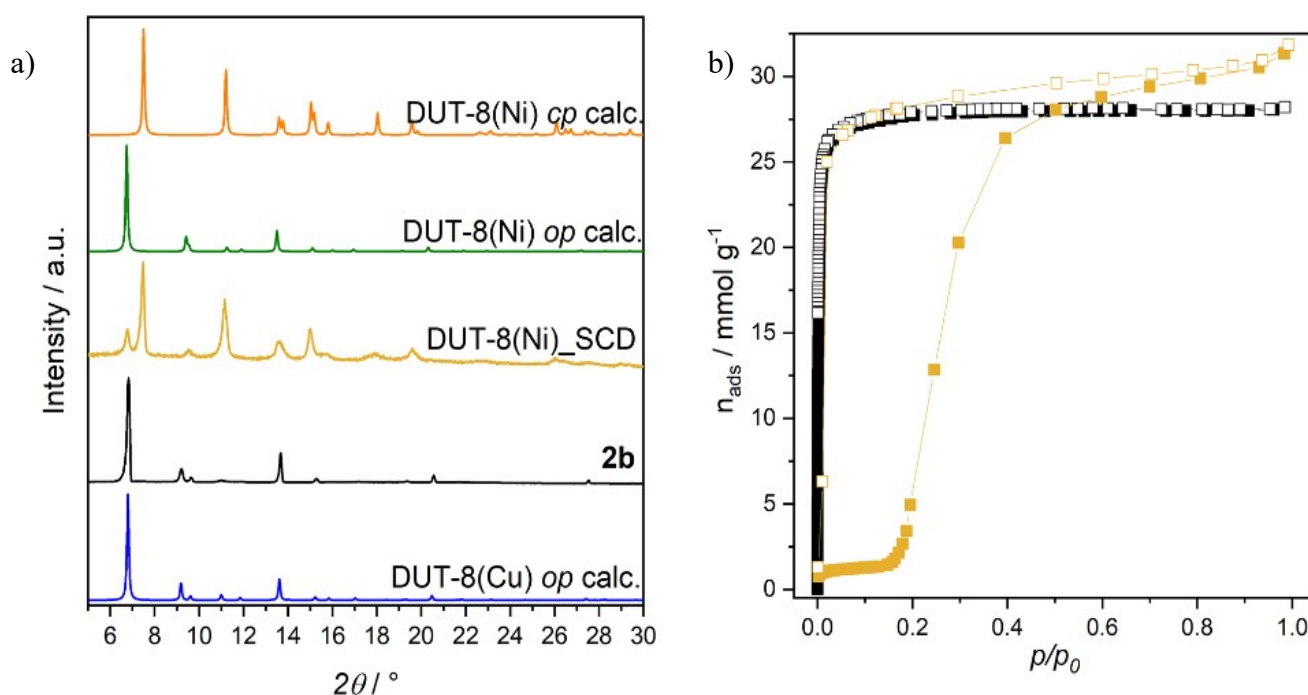


Fig. S3.2. a) PXRD patterns of the macro-sized particles, supercritically dried from acetone: DUT-8(Ni) (yellow) and **2b** (black) in comparison with PXRD calculated for DUT-8(Cu)_op (blue), DUT-8(Ni)_op (green) and DUT-8(Ni)_cp (orange); b) N₂ physisorption at 77 K on macro-sized DUT-8(Ni) particles supercritically dried from acetone (yellow) and **2b** (black). Solid symbols – adsorption, empty symbols – desorption.

As it can be seen from Figure 3.2, the same desolvation procedure applied to the macro-sized DUT-8(*M*) particles containing Cu or Ni results in different phases: mainly cp phase of DUT-8(Ni) and pure op phase of DUT-8(Cu).

S4 Crystal structure

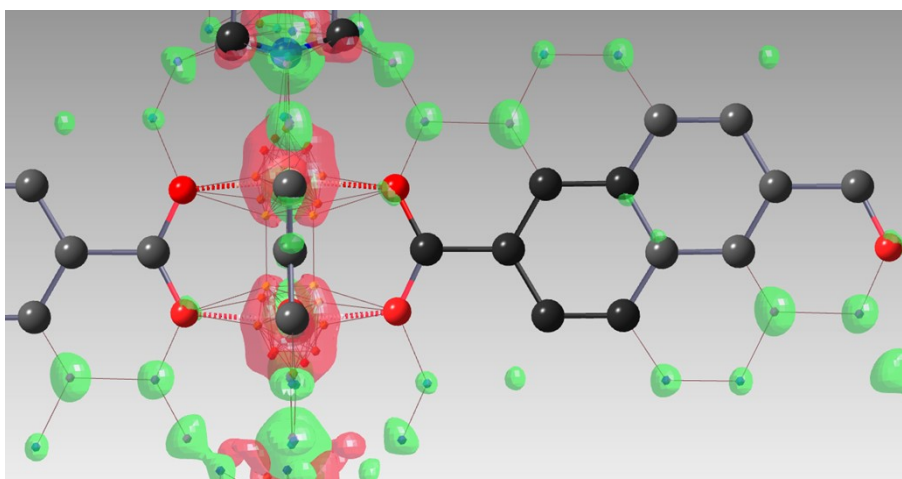


Figure S4.1 Difference Fourier map of the DUT-8(Cu) single crystal indicates localised maxima of the electron density (green) in addition to the main structural motif of the linker and cluster (in black). When connected (thin lines), they resemble a different linker orientation and a disorder along the *c*-axis.

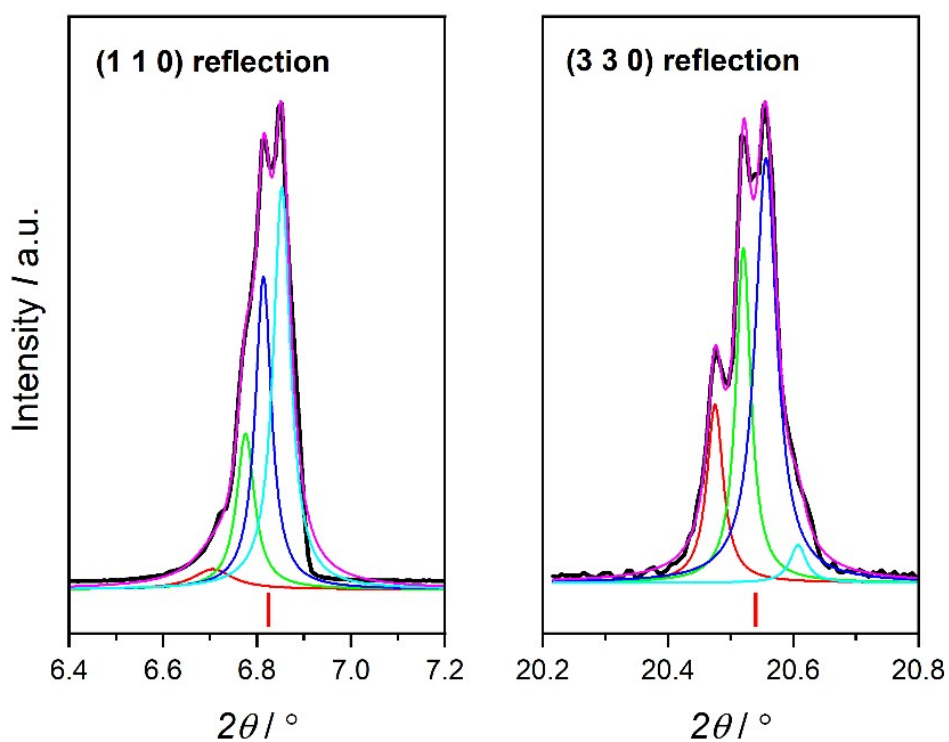


Figure S4.2. Diffraction peaks splitting in **2b**.

S5 Adsorption behaviour

Table S5.1. Adsorption characteristics of the investigated samples.*

Sample name	$n_{\text{ads}}(\text{N}_2, 77\text{K}),$ mmol g^{-1}	α_{max}^{**}	$n_{\text{ads}}(\text{CO}_2, 195\text{K}),$ mmol g^{-1}	α_{max}
1a	29.3	1	23.47	0.93
2a	9.82	0.33	9.27	0.37
2b	28.2	0.96	22.11	0.88

** $\alpha_{\text{max}} = n_{\text{ads}}(\text{experimental}) / n_{\text{ads}}(\text{theoretical})$, n – amount of substance adsorbed.

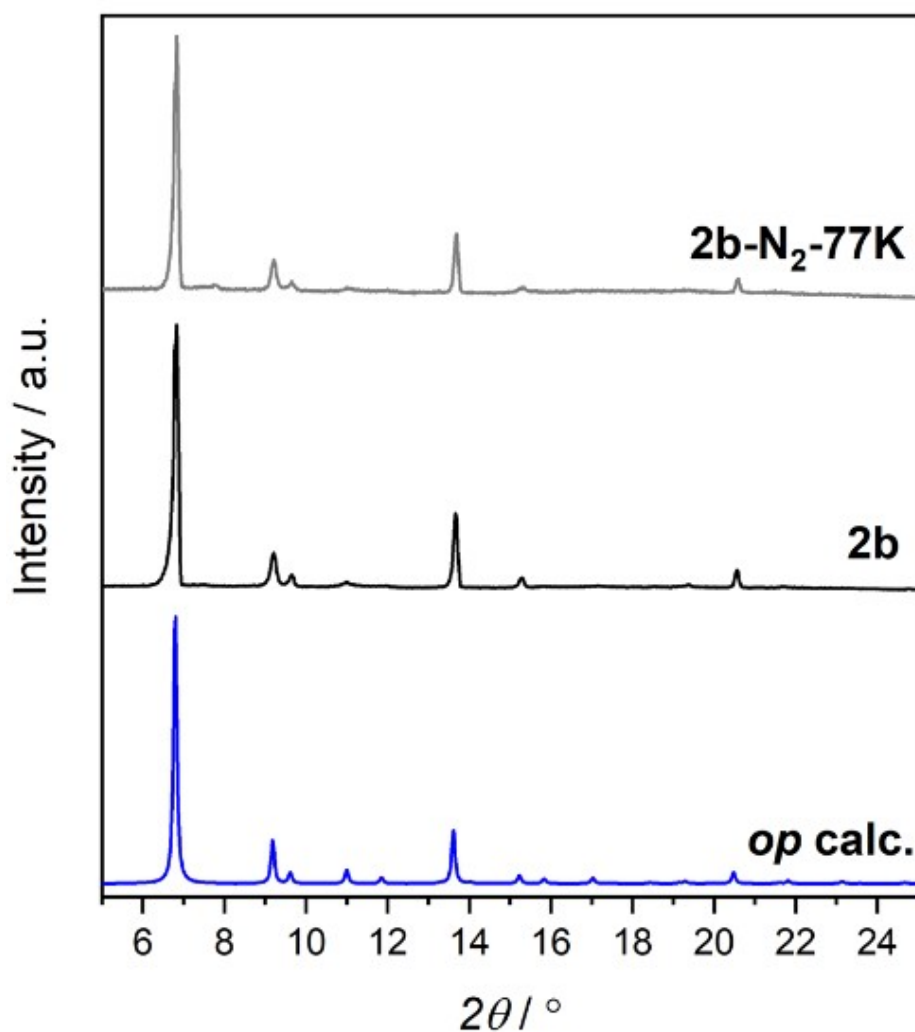


Fig. S5.1. PXRD patterns of **2b** before (black) and after N₂ physisorption at 77 K (gray).

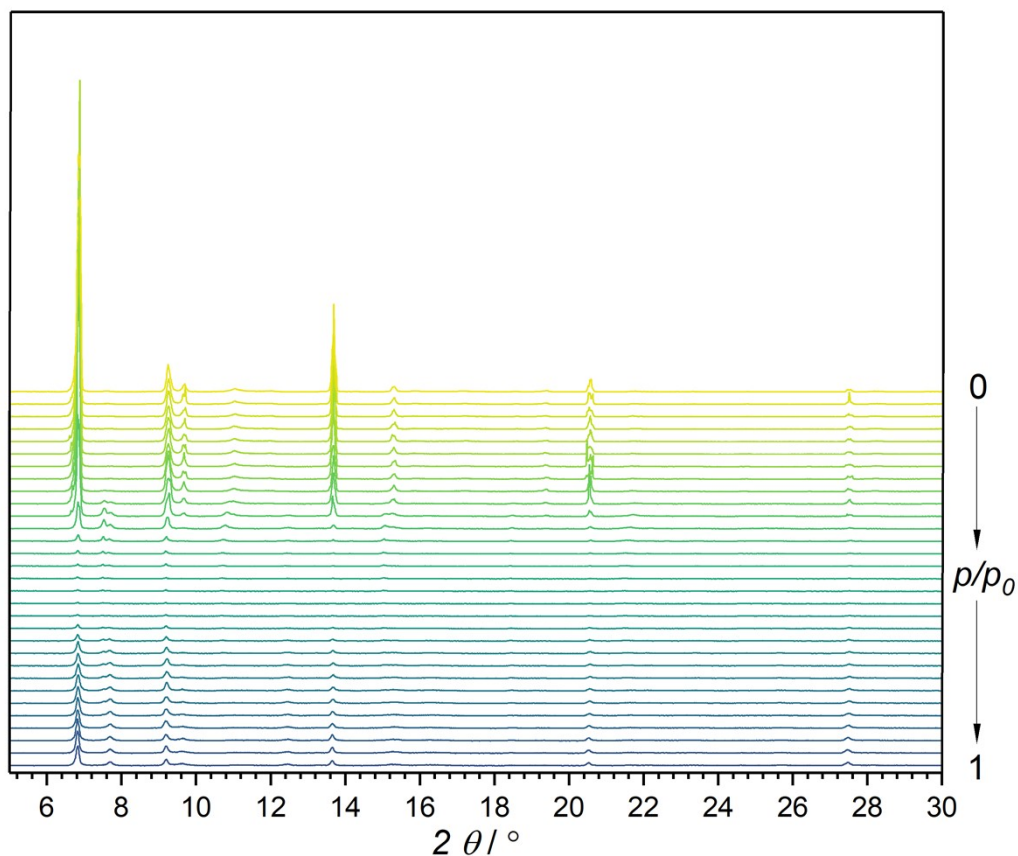


Fig. S5.2. PXRD patterns collected *in situ* upon CO₂ adsorption at 195 K on **2b**.

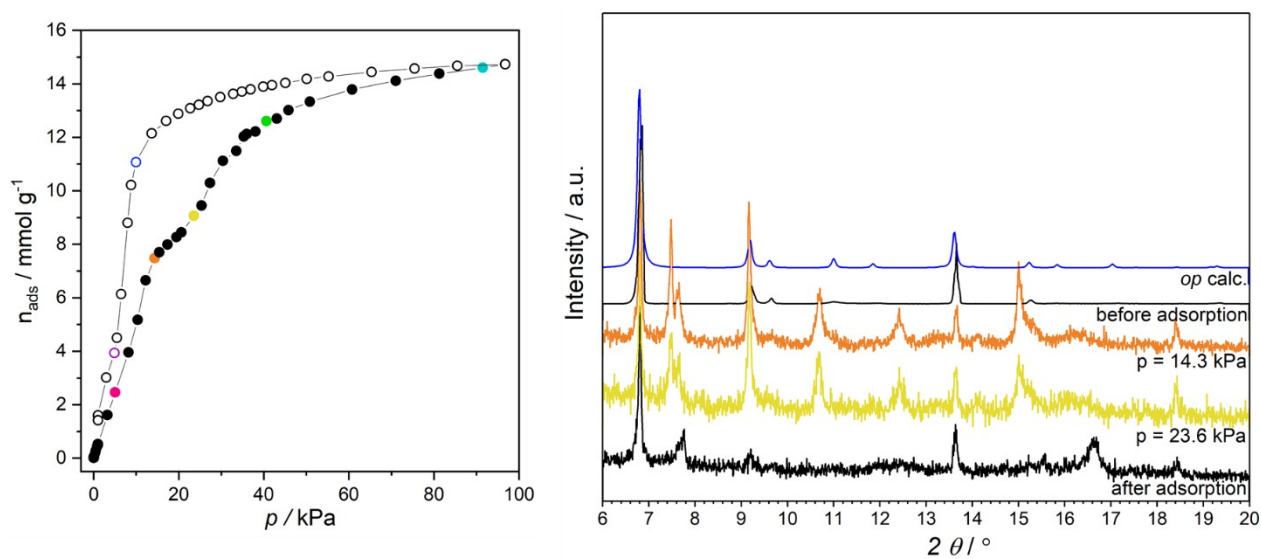


Fig. S5.3. *In situ* CO₂ physisorption isotherm at 195 K and some selected PXRD patterns for **2b**.

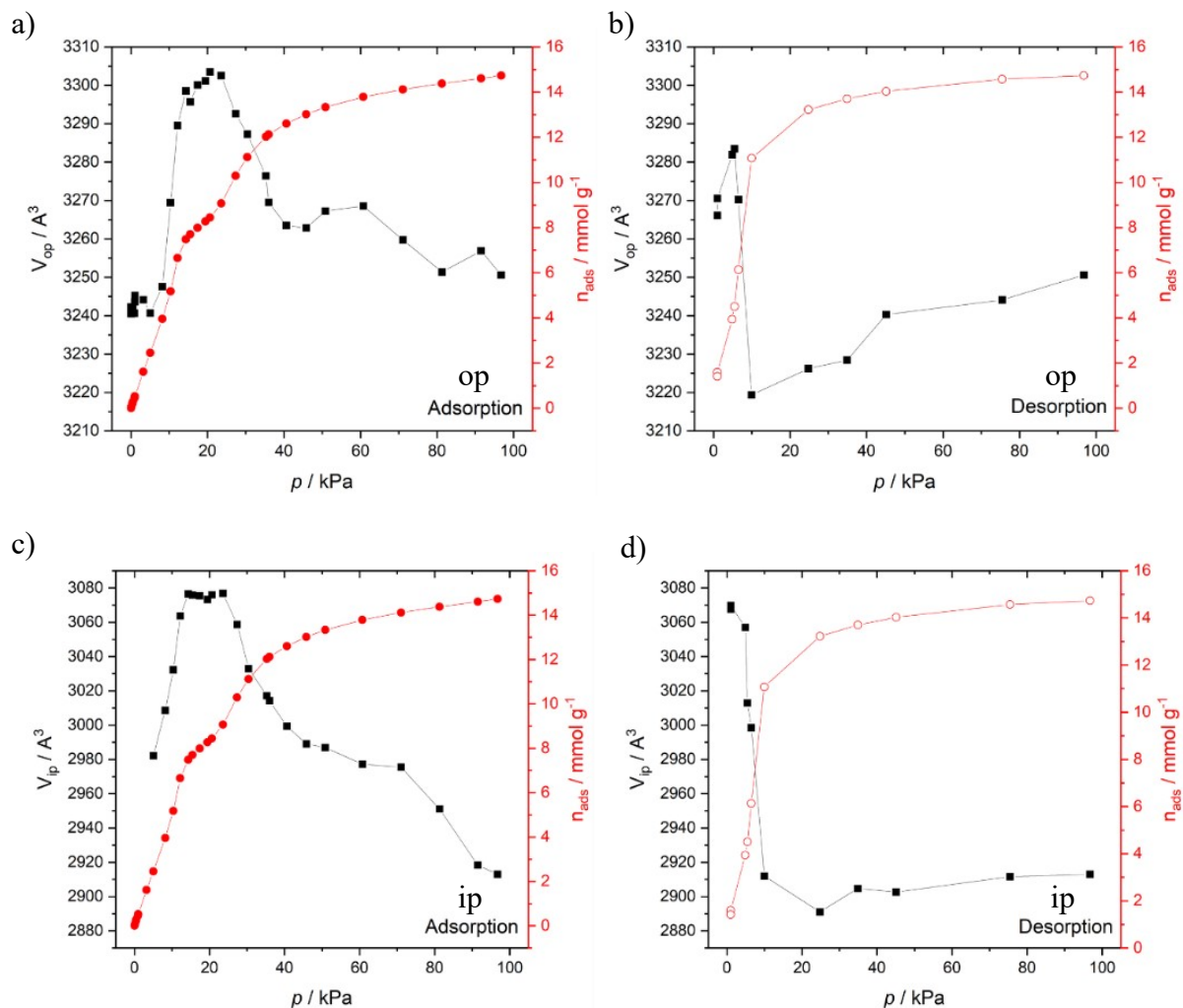


Fig. S5.4. Unit cell volume change of the open pore (op) and intermediate pore (ip) phases upon adsorption (a, c) and desorption (b, d) of CO₂ at 195 K, performed on **2b**.

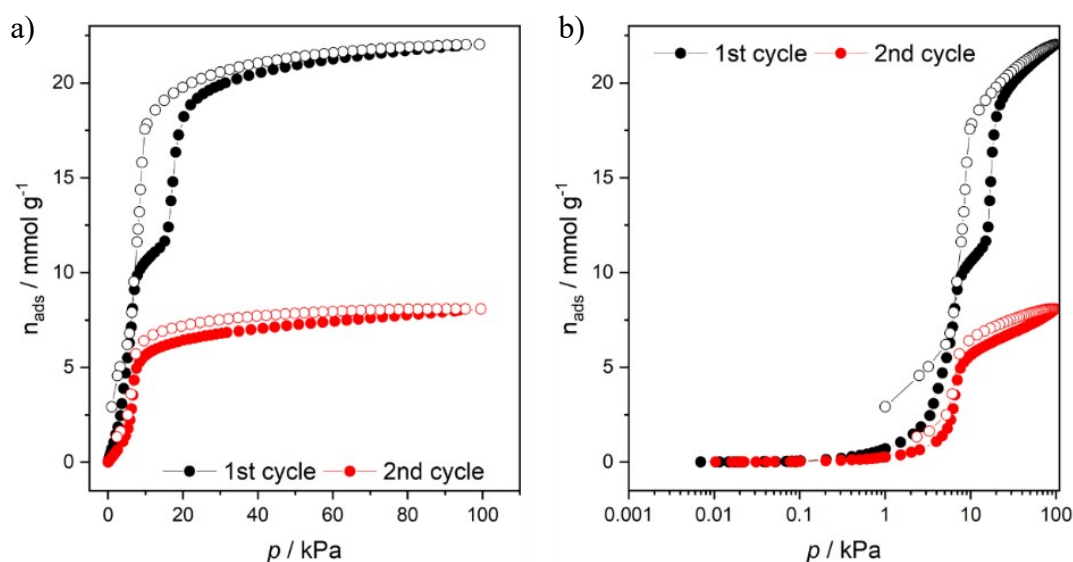


Fig. S5.5. Cyclic adsorption/desorption of CO₂ at 195K for **2b**: (a) linear scale; (b) logarithmic scale. Black – 1st adsorption/desorption cycle, red – 2nd adsorption/desorption cycle. Solid symbols – adsorption, empty symbols – desorption.

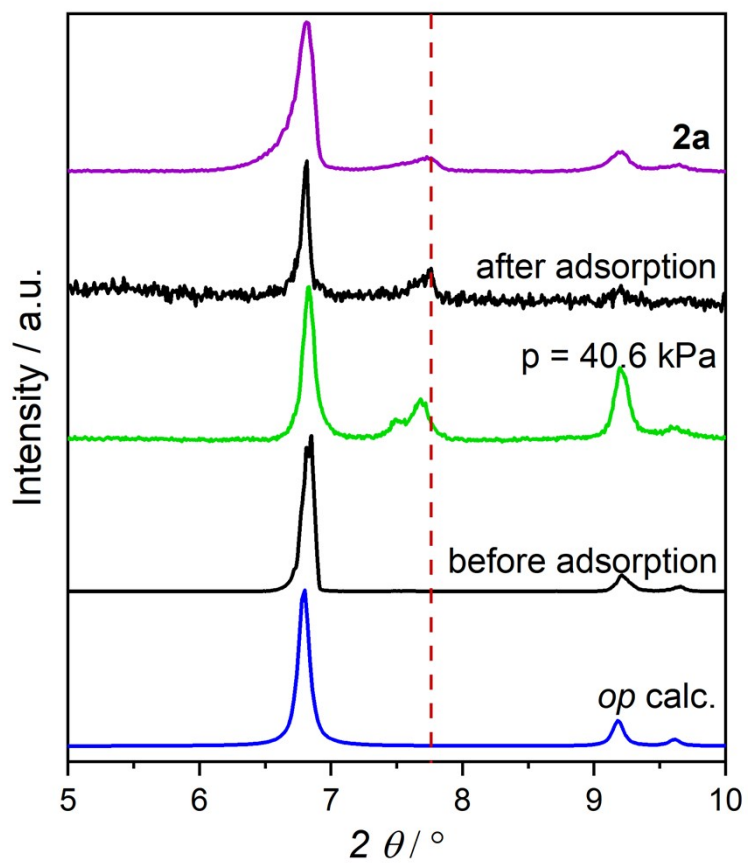


Fig. S5.6. PXRD patterns of: **2b** at 298 K before *in situ* adsorption were measured (black) **2b** loaded with CO₂ at 195 K at $p = 40.6$ kPa (green), **2b** evacuated at 298 K after CO₂ adsorption/desorption (black), of **2a** (violet). Red line marks the position of the peak of the new phase.

S6 Cluster optimisation

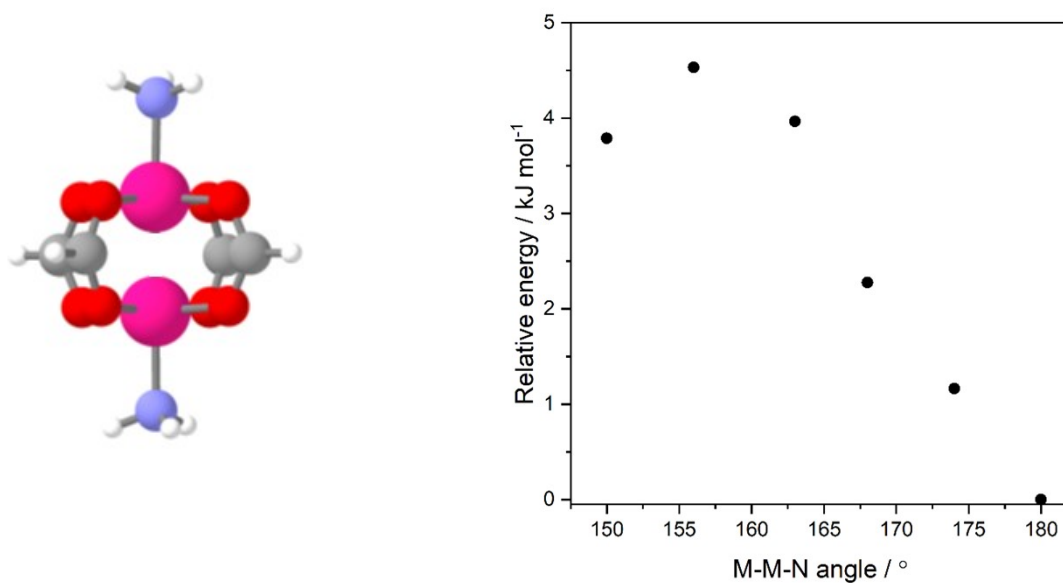


Fig. S6.1 Structure of the Cu paddle wheel cluster molecular analogue (left). The constrained geometry scans of the Cu-Cu-N angles in the paddle wheel cluster (right).

S7 Thermal analysis

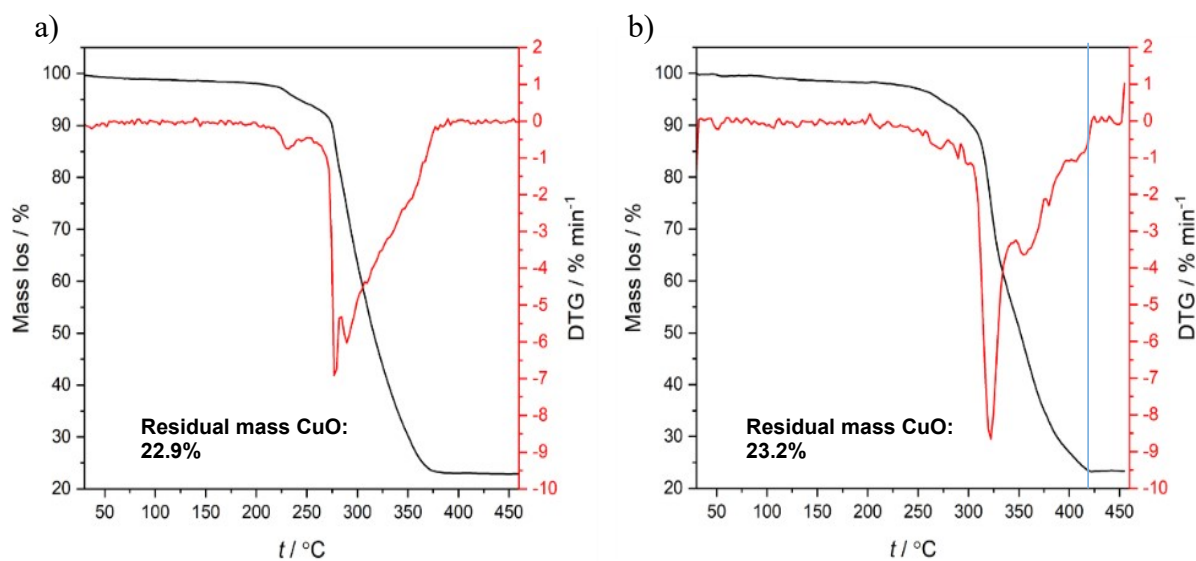


Fig. S7.1 Thermogravimetric analysis (black) / differential thermogravimetric analysis (red) curves of the **1a** (a) and **2b** (b).

In situ thermo-PXRD

Thermo-PXRD measurements were performed on an Empyrean diffractometer (PANALYTICAL GmbH) equipped with a high-temperature chamber in the temperature range of 298 - 723 K with a heating rate of 5 K min⁻¹ under nitrogen flow. The temperature steps are 25 K and the equilibration time at a given temperature is 30 min. The powder patterns were taken in reflection mode using copper K α_1 radiation and a wavelength of 1.5406 Å.

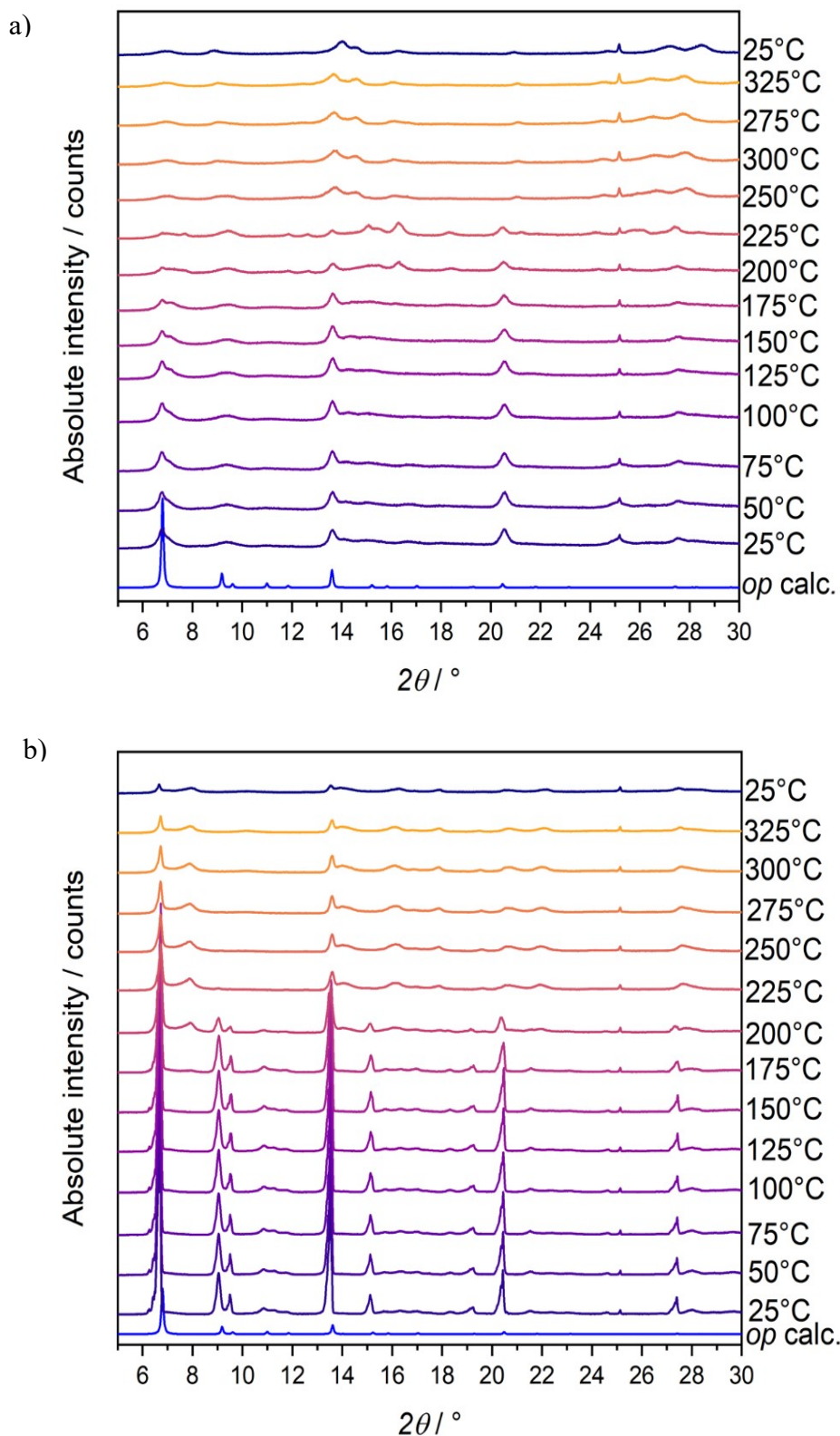


Figure S7.2. Thermo-PXRD patterns of **1a** (a) and **2a** (b) collected upon heating in an inert gas atmosphere (N₂ flow).

Table S7.1 Ratio of 2,6-ndc to dabco in **1a** and **2b** found after thermal treatment in the inert gas atmosphere at elevated temperatures. The ratios were calculated from ^1H NMR spectra obtained from the digested samples.

2,6-ndc: dabco	Initial	200 °C	240 °C	300 °C	340 °C	Vacuum 160 °C
1a	1:0.95	1:0.723	1:0.597	1:0.306	1:0.291	
2b	1:0.99	1:0.849	1:0.417	1:0.427	1:0.243	1:0.96

S8 ^1H NMR spectroscopy

Before measurements, the samples **1a**, **2a** and **2b** were digested in the mixture of DMSO- d_6 (0.6 ml) and deuterium chloride solution (2 drops) under ultrasonication. The spectra were measured using the Bruker spectrometer at 300 MHz.

Based on the chemical formula of the DUT-8(Cu) ($[\text{Cu}_2(2,6\text{-ndc})_2\text{dabco}]_n$), the theoretical ratio of the peaks at 8.65 ppm (2H, 2,6-naphthalene dicarboxylate) and 3.55 ppm (12H, dabco) of the linker to pillar should be 1:3.

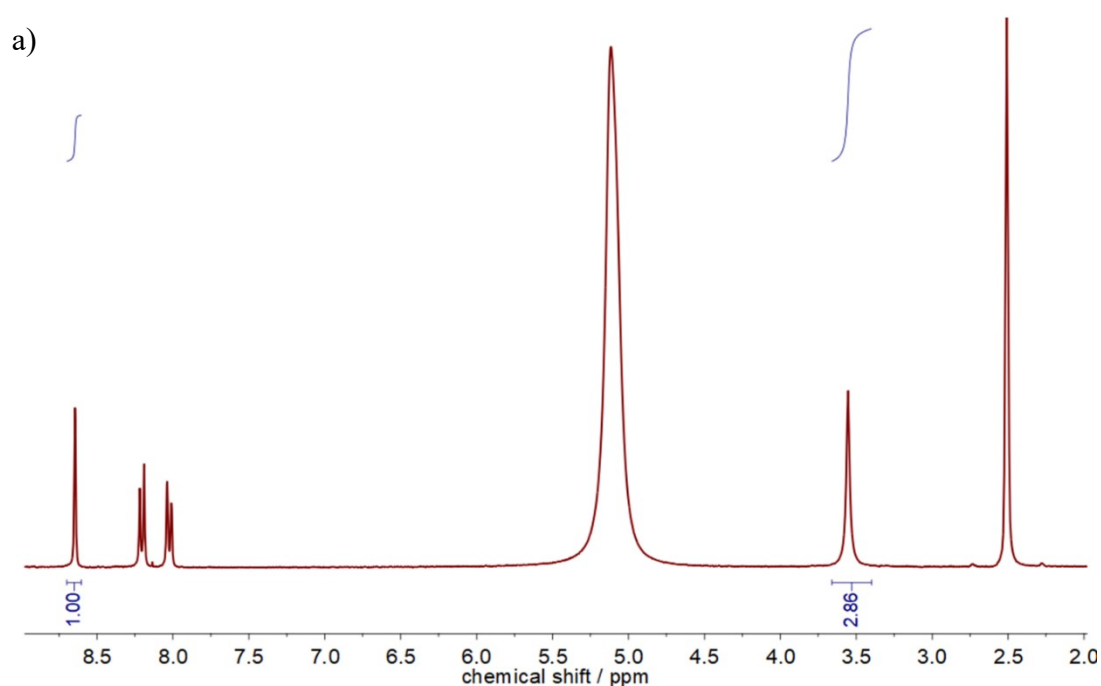


Fig. S8.1 a) ^1H NMR spectra of **1a**.

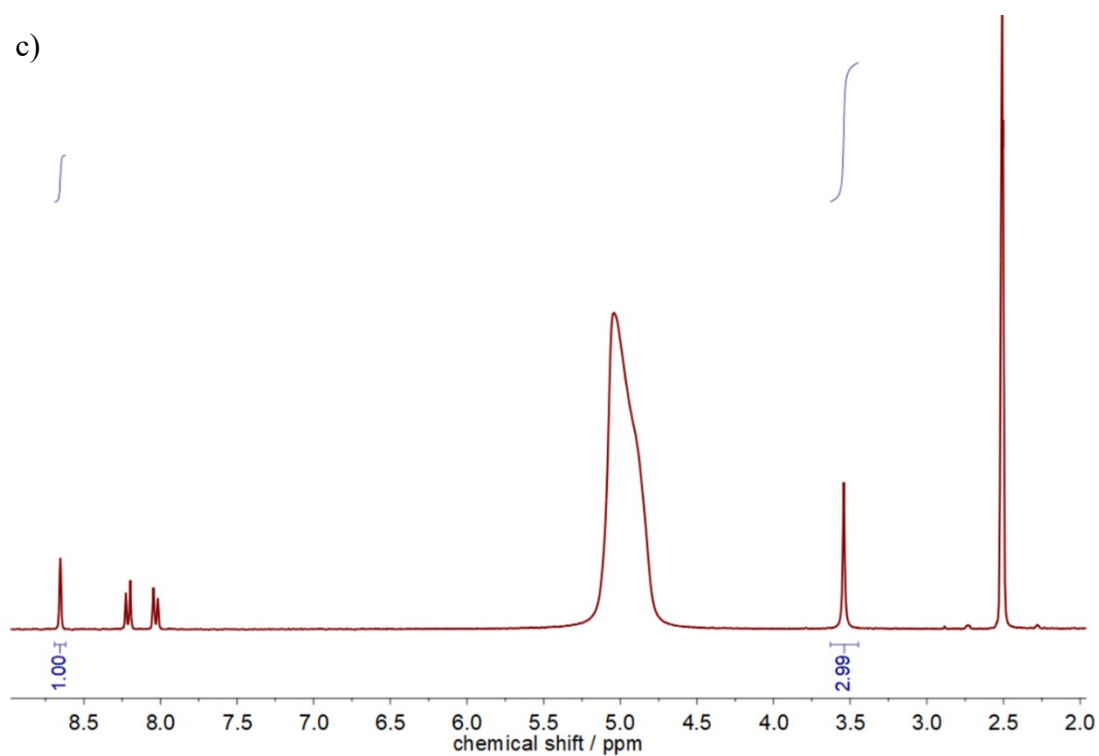
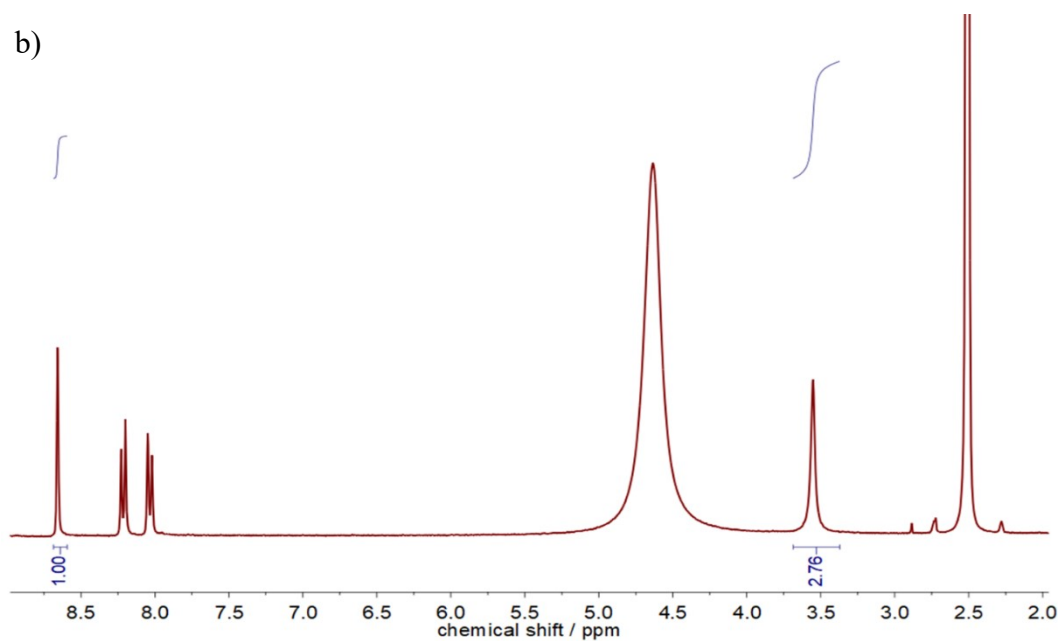


Fig. S8.1 a-b) ^1H NMR spectra of **2a** (b) and **2b** (c).

Table S8.1 Ratio of 2,6-ndc to dabco in **1a**, **2a**, and **2b** found after desolvation. The ratios were calculated from ^1H NMR spectra shown in Fig. S8.1 and obtained from the digested samples.

Ratio	1a	2a	2b
2,6-ndc : dabco	1:0.95	1:0.92	1:0.99

References

1. N. Klein, H. C. Hoffmann, A. Cadiou, J. Getzschmann, M. R. Lohe, S. Paasch, T. Heydenreich, K. Adil, I. Senkovska, E. Brunner and S. Kaskel *J. Mater. Chem.*, 2012, **22**, 10303.
2. N. Klein 2012, *PhD thesis*, Department of Inorganic Chemistry, Technische Universität Dresden.